Science of the Total Environment 739 (2020) 139990

Contents lists available at ScienceDirect

Science of the Total Environment

journal homepage: www.elsevier.com/locate/scitotenv

Raman spectra and surface changes of microplastics weathered under natural environments

Mingtan Dong [a,c], Qiaoqiao Zhang [a,c], Xinli Xing [a], Wei Chen [a], Zhenbing She [b,d,*], Zejiao Luo [a,**]

[a] School of Environmental Studies, China University of Geosciences, Wuhan 430078, China
[b] State Key Laboratory of Biogeology and Environmental Geology, China University of Geosciences, Wuhan 430078, China
[c] School of LiSiguang, China University of Geosciences, Wuhan 430074, China
[d] School of Earth Sciences, China University of Geosciences, Wuhan 430074, China

HIGHLIGHTS

- Raman spectra of weathered microplastics differ greatly from standard spectra.
- A preliminary Raman database of weathered microplastics is established.
- Surface C and O elemental maps of the weathered microplastics are complementary.

GRAPHICAL ABSTRACT

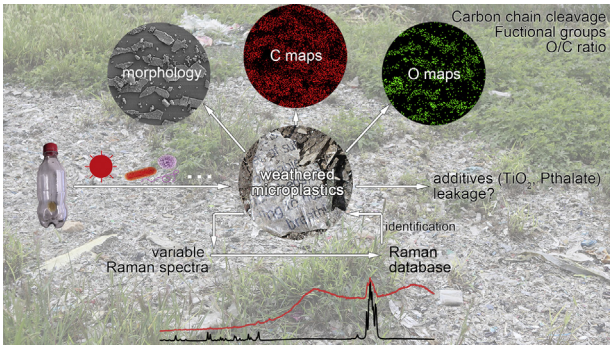

ARTICLE INFO

Article history:
Received 7 April 2020
Received in revised form 3 June 2020
Accepted 3 June 2020
Available online 05 June 2020

Editor: Damia Barcelo

Keywords:
Microplastics
Raman spectra
Weathering
Surface changes
Fourier transform infrared spectrometry

ABSTRACT

Raman spectroscopy can be used to effectively analyze submicron- to microsized microplastics, but Raman spectra of weathered microplastics commonly show deviations from those of unweathered microplastics and are often affected by fluorescence. However, studies of weathering-induced surface changes in microplastics have been limited to laboratory simulations. To systematically study Raman spectra and surface changes of microplastics weathered under natural environments, we collected microplastics from sediments around waste plastics processing and recycling industries in Laizhou City, Shandong Province, East China. Raman spectra of weathered microplastics differ greatly from standard spectra of unweathered plastic material. Peaks in the Raman spectra of weathered microplastics are weakened and even invisible. A preliminary Raman database of weathered microplastics (RDWP) including 124 Raman spectra of weathered microplastics was built to accurately identify microplastics in natural environments, and it is open to all users. FTIR spectroscopy revealed the presence of oxygen-containing functional groups and C═C bonds related to oxidation and chain scission. SEM showed that weathered microplastics had rough surfaces and that PP was more easily fractured than PE. Complementary C and O elemental maps suggested that the O/C ratio is a potential indicator of oxidation degree. EDS revealed titanium on PET and PVC surfaces, which is related to titanium dioxide typically used as a light-blocking aid. Our data document that Raman spectroscopy has great potential in the identification of naturally weathered microplastics and that combined spectral and elemental analyses can be useful in deciphering the degradation processes of microplastics under natural conditions.

* Correspondence to: Zhenbing She, State Key Laboratory of Biogeology and Environmental Geology, School of Earth Sciences, China University of Geosciences, 388 Lumo Road, Wuhan 430074, China.
** Correspondence to: Zejiao Luo, School of Environmental Studies, China University of Geosciences, 68 Jincheng Street, Wuhan 430078, China.
E-mail addresses: zbsher@cug.edu.cn (Z. She), zjluo@cug.edu.cn (Z. Luo).

https://doi.org/10.1016/j.scitotenv.2020.139990
0048-9697/

Capsule: Raman spectra of weathered microplastics differ greatly from standard spectra. A Raman database of weathered microplastics is established. Surface changes of weathered microplastics were systematically studied.

1. Introduction

Microplastics (Thompson et al., 2004), plastic debris smaller than 5 mm, have raised widespread concern in society and the scientific community. Currently, the upper size limit of microplastics is defined as 5 mm (Thompson et al., 2004), but the lower size limit has not yet been accurately defined (Dehaut et al., 2019). Studies have shown that the abundance of micrometer-sized microplastics in environmental samples is high (Brandon et al., n. d.; Imhof et al., 2016; Song et al., 2018; Vianello et al., 2019; Zuccarello et al., 2019) and that small-sized microplastics are easily ingested by organisms (Chain, 2016; Roch et al., 2019) and have significant toxic effects (Gray and Weinstein, 2017; Strungaru et al., 2019). When researching microplastics in environmental samples, we need to pay attention to the smaller particle sizes and identify accurate polymer types (Dehaut et al., 2019; Dong et al., 2020b; Miraj et al., 2019).

Raman spectroscopy can detect microplastics with a size of 1 μm (Ossmann et al., 2018) and is considered to be effective when analyzing small-sized microplastics (Pico et al., 2019; Schwaferts et al., 2019; Sobhani et al., 2019; Zuccarello et al., 2019). However, due to the resonance fluorescence phenomenon inherent in Raman scattering, Raman spectroscopy is susceptible to strong fluorescence interference when applied to the detection of microplastics, especially when detecting plastic samples that are colored, weathered in the environment or adhered with organic matter residues (Dehaut et al., 2019; Kappler et al., 2016; Zarfl, 2019). Therefore, considering that the Raman spectra of weathered microplastics are prone to change and that there is no specific Raman database of weathered microplastics, it is essential to build a spectral database of weathered plastics and use it when identifying unknown microplastics in environmental samples.

In addition, the ability to absorb organic pollutants (Koelmans et al., 2013) and heavy metals (Dong et al., 2020b; Gao et al., 2019) is known for microplastics, especially aged or weathered microplastics, which are considered to have enhanced adsorption (Huffer et al., 2018; Liu et al., 2019a; Zhang et al., 2018). Studies about the surface changes on aged or weathered plastic surfaces are mostly performed in the lab (Gewert et al., 2015; Tosin et al., 2012) via simulated photooxidation (Jelle and Nilsen, 2011) or chemical oxidation (Liu et al., 2019b). However, the degradation process of weathered microplastics in natural environments is more complicated than that in lab simulations. Researching the surface changes of microplastics weathered in the field is important to understand the persistence of microplastics pollution and the origin of small-sized microplastics.

Therefore, to systematically study the changes in the Raman spectra, physical morphology and chemical composition of the surface of weathered microplastic debris under natural environments, one of the largest centers of waste plastics processing and recycling industries in China was selected as the study area. We sampled the sediments in a dry ditch of the study area and picked up the weathered microplastic debris. Raman spectra were obtained for identifying polymer types and building the Raman Database of Weathered Plastics (RDWP). Fourier transform infrared spectrometry (FTIR) was used to analyze the changes in surface functional groups. Scanning electron microscopy-energy dispersive X-ray spectroscopy (SEM-EDS) was used to study the changes in surface morphology and elemental composition.

2. Methods

2.1. Study area and sample collection

The study area is located in the Luwang Area of Shahe Town, Laizhou City, Shandong Province, China (Fig. S1a, b). Many waste plastics processing and recycling industries have gathered in this area since the 1980s. The enterprises in this area were mostly family workshops and lacked environmental protection equipment and capabilities; in the process of disposing of waste plastics, a large number of plastics were placed directly on the ground with no cover and exposed to air, and wastewater and waste gas were randomly discharged into the environment. Waste plastics recycling industries have imported a large number of waste plastics from developed countries all over the world. Thus, the microplastics are not only from one city but, rather, represent a miniature of plastics in the world.

Samples were collected along the Zhenzhu River in the study area in August 2018 (Table S1). A large amount of (micro)plastic debris can be seen in surface sediments (Fig. S1c, d). We sealed the sediment samples in glass bottles and preserved them in darkness, and we randomly selected 155 microplastic debris samples (Fig. S2) from the sediment samples and studied their surface characteristics. The microplastic debris was directly removed from the sediments with tweezers and naturally air dried. A part of the attached dirt was naturally removed from the surface in the process of air drying, and additional residues were removed with a dust blower ball and Delicate Task Wipes (KIMTECH) carefully and gently. Detailed information about the study area and sample collection are given in the SI.

2.2. Confocal micro-Raman spectroscopy

Micro-Raman microscopy was conducted on selected microplastic targets using a WITec alpha300-R confocal Raman imaging microscope at the State Key Laboratory of Biogeology and Environmental Geology, China University of Geosciences (Wuhan). The instrument was equipped with a 532-nm wavelength laser and set at a power between 2 and 10 mW (usually 5 mW). Raman spectra were obtained at variable magnifications of 10× to 100× and hence at variable spatial resolutions of up to 360 nm. The Raman spectra were collected in the 200–3500 cm^{-1} range using 600 lines per millimeter grating, which yielded a spectral resolution of 4 cm^{-1}. The integration time was 1–10 s (usually 5 s), and the cumulation number was 1–10 times (usually 4). To obtain the spectrum with low fluorescence and the highest possible quality, we used different Raman settings for the same spot or collected multiple spectra at different spots on the same sample. A total of 155 spectra of weathered microplastic debris and 18 spectra of standard plastics were collected. The standards were purchased from "Taobao.com" or derived from plastic packaging for food, daily necessities, and laboratory plastic consumables.

2.3. FTIR analysis

An FTIR (Nicolet iS50 FT-IR, Thermo Scientific) equipped with a pluggable attenuated total reflection (ATR) accessory was used to identify the microplastics that could not be identified by Raman spectroscopy and to analyze the changes in the functional groups of the surface. The FTIR spectra were collected in the 650–4000 cm^{-1} range. A total of 54 FTIR spectra were collected with a cumulative number of 20 times and a spectral resolution of 0.482 cm^{-1}.

2.4. Spectra analysis

The KnowItAll Informatics System 2018 (Bio-Rad Laboratories) was used to analyze the Raman spectra. The software can perform spectral searches, spectral identification, functional group analysis, etc., and has spectral data management capabilities, allowing users to build spectral databases by themselves. First, the spectra of the standards were built as a Raman Database of Standard Microplastics (RDSP) separately in KnowItAll. Then, the RDSP was used as one of the searched databases, and the spectra of weathered microplastics were matched and identified. Finally, the spectra of weathered microplastics were built as the Raman database of weathered microplastics (RDWP).

2.5. SEM-EDS analysis

SEM was conducted with a Tescan VEGA3 SEM in the State Key Laboratory of Biogeology and Environmental Geology at CUG-Wuhan. Analyses were performed on microplastics under a vacuum pressure of 10^{-3} mbar with a 0.25 nA electron beam accelerated at 10 keV, and the X-rays were collected on an electronically cooled Oxford Instrument AztecOne EDS XT detector. The surface of the microplastic debris was presprayed with platinum to improve electrical conductivity. In addition, the EDS was used to obtain the elemental composition of microplastic targets with spot analysis, line scan and mapping modes. A total of 40 microplastic debris samples were analyzed by SEM-EDS. The O/C ratio was calculated as the atomic ratio of oxygen and carbon.

3. Results and discussion

3.1. Raman spectra of weathered microplastics

The Raman spectra of weathered microplastics were distinctly different from the spectra of fresh standard samples (Figs. 1, S3–S6). The Raman spectra (Fig. 1a–d) were identified as PE based on the two peaks at 2846 and 2881 cm^{-1} and were also verified by ATR-FTIR. The relative intensities of the 2846 and 2881 cm^{-1} peaks in the Raman spectra changed significantly after weathering (Fig. 1b–e). The peaks at 2846 and 2881 cm^{-1} of weathered microplastics were relatively weak, and there was a broad and strong band in the range of 2100–2200 cm^{-1} (Fig. 1b–d). In addition, the stretching vibrations of C—C at 1060 and 1127 cm^{-1} and the bending vibrations of CH_2 at 1293 and 1438 cm^{-1} were distinct in the Raman spectra of sta-1 and wea-27 (Fig. 1a, b), but these peaks were not visible in the Raman spectra of wea-17 and wea-24 (Fig. 1c, d).

Similarly, PP was identified by several peaks at 2800–3000 cm^{-1} in the Raman spectrum (Fig. S4) and were also verified by ATR-FTIR. However, the peaks of CH_2 stretching vibration between 2800 and 3000 cm^{-1} in some spectra were relatively weak, and a broad and strong band was also observed in the range of 2100–2200 cm^{-1} (Fig. S4). The peaks of CH_2 stretching vibration in the spectra of weathered PET were relatively weak (Fig. S5). Additionally, the Raman spectra of weathered PVC microplastic debris were inconsistent with the standard spectra (Fig. S6). Except for the attenuation of CH_2 stretching vibration, the peaks of C—Cl vibration in some spectra of weathered PVC were weak as well (Fig. S5), which indicates the dechlorination in the weathering process of PVC.

We collected multiple spectra on different depths in the same spot with the help of the confocal function of Raman microscope. The spectra collected at different depths were generally consistent except for the change in Raman intensity (Fig. S7), which indicates that the possible disturbance from the organic matter attached on the surface was minimized.

The significant differences between the Raman spectra of weathered microplastics and the standard spectra have been widely reported in many studies (Di et al., 2019; Huang et al., 2019; Li et al., 2019; Wang et al., 2018; Xiong et al., 2018) and may lead to the inaccurate identification of certain microplastics. Specifically, the weakened stretching vibrations of methyl, methylene and methine at 2800–3000 cm^{-1} and a broad and strong band at 2100–2200 cm^{-1} are universally displayed in many different studies (Di et al., 2019; Huang et al., 2019; Li et al., 2019; Wang et al., 2018; Xiong et al., 2018). Thus, given the inconsistency between the spectra of standard samples and the spectra of weathered samples (Figs. 1, S3–S6), the visible and valid Raman peaks for identifying weathered microplastics are listed in Table 1, and it is crucial to build a Raman database of weathered microplastics.

Raman mapping developed by WITec (Kappler et al., 2016; Sobhani et al., 2019) is an efficient method and has been used to identify microplastics. Raman mapping obtains the spectra of all points in a

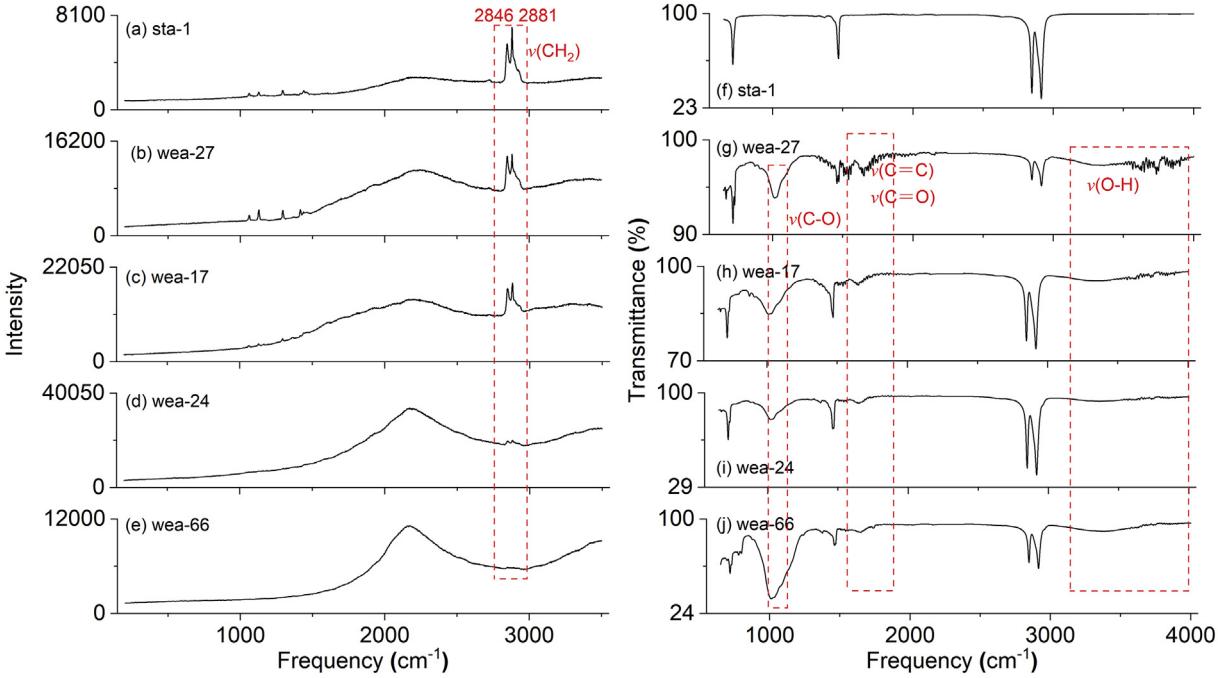

Fig. 1. Raman spectra (left) and ATR-FTIR spectra (right) of PE microplastic debris. All spectra were not baseline subtracted.

Table 1
Visible and valid Raman peak combinations for identifying weathered microplastics.

Polymer types	Raman peaks (cm^{-1})
PE	2846(CH_2), 2881(CH_2)
PP	2839(CH_2), 2881(CH_2), 2904(CH_2), 2960(CH_3)
PET	1612(phenyl), 1726(C=O), 3082(C—H of phenyl)
PVC	638 (C—Cl)[a], 694(C—Cl)[a], 2911(CH_2)

[a] The vibration of C—Cl at 638 and 694 cm^{-1} was invisible in certain Raman spectra of weathered PVC.

plane with a certain spatial resolution and maps the distribution of microplastics by postprocessing the spectrum. Raman mapping can identify microplastics from the matrix by integrating the mutual peaks of the polymer (such as 2800–3100 cm^{-1}) and identify the specific polymer type by integrating the particular peaks. It has the potential to detect small-sized microplastics, but the detection and quantification method based on Raman mapping is time consuming and has not yet been standardized. This technology was successfully used to identify microplastics as small as 0.1 μm (Sobhani et al., 2020) and distinguish microplastics from the sand background (Sobhani et al., 2019). However, the microplastics used for Raman mapping were fresh standard samples rather than weathered microplastics (Sobhani et al., 2019). The range of 2800–3100 cm^{-1} was used as the mutual peak (Sobhani et al., 2019), but the peak intensity of weathered microplastics in this range decreased significantly (Figs. S3–S6). Specifically, the peaks at 694 cm^{-1} for PVC, 1059 cm^{-1} for PE and 402 cm^{-1} for PP, which were used for acquiring different polymer types (Sobhani et al., 2019), were weakened in the weathered microplastics (Figs. S3–S6) and could not be distinguished from the fluorescence background. Therefore, it is necessary to further study the application of Raman mapping technology in detecting weathered microplastics in environmental samples; in particular, we need to select the peaks cautiously for integration.

3.2. The building of a preliminary Raman database

The Raman Database of Standard Microplastics (RDSP) contains 18 spectra of 8 polymer types (Table 2). ATR-FTIR spectra were collected for 20 debris samples unrecognized by Raman, but 10 samples remain unidentified. The combined results of Raman and ATR-FTIR identification show that the microplastic debris in our study area is mainly PE and PP, accounting for 45.2% and 32.9%, respectively, of the total. PET and PVC microplastic debris accounted for 6.45% and 4.52%, respectively. In addition, 6.45% of the microplastic debris was not identified. The high percentage of PE and PP is related to the polymer types of recycling plastics in this waste plastics processing and recycling industries area.

Among the 135 Raman spectra that could be identified, we selected 124 spectra with distinct peaks to build a preliminary Raman database of weathered microplastics (RDWP). The number of spectra for each polymer type is given in Table 2. These 135 identified spectra were mostly utilized to best address the variability and uncertainty of the spectra of weathered plastics in the environment, and we need to balance the variety and accuracy of RDWP at the same time. The criteria of selection are that (1) the included Raman spectra must have at least one clearly specific peak, such as the peaks listed in Table 1; (2) the spectra with inconsistent peaks or large fluorescence background were excluded. Eleven spectra were excluded in the RDWP mainly due to inconsistencies in the standard spectra, such as those displaying a prominent fluorescence background or inconsistent peaks. Fluorescence might originate from the surface changes and the attached environmental organic matter residues. Given PVC as an example (Fig. S6), wea-49 shows an inconsistent peak at 1595 cm^{-1}, wea-156 shows a large fluorescence background, and wea-106 (identified by FTIR) does not show any informative peak. In this case, the Raman spectra of wea-49 and wea-106 are excluded in RDWP. We believe that the building of RDWP will improve the matching score between the Raman spectra of weathered microplastics and the standard spectra, but the effect of RDWP in identifying weathered microplastics needs to be verified by other researchers.

Table 2
Spectra numbers of the identified microplastic debris.

	RDSP[a]	Raman identification	ATR-FTIR identification	RDWP[b]
Total	18	155	20	124
PE	2	67	3	62
PP	3	47	4	44
PET	6	10	0	10
PVC	2	6	1	4
PS	1	0	1	0
PC	1	1	0	1
PA	2	3	1	2
ABS	0	1	0	1
NC	1	0	0	0
NI[c]	0	20	10	0

[a] Raman Database of Standard Microplastics.
[b] Raman Database of Weathered Microplastics.
[c] No Identification.

The database and raw data of all spectra are given by Mendeley data (Dong et al., 2020c) and open to all users. The database will be updated online with Mendeley data, and we will provide additional spectra in the following versions.

3.3. Changes in surface functional groups

Raman spectroscopy can be used to identify polymer types, but it is difficult to further obtain information about the changes in the chemical composition of the polymer surfaces. However, Raman spectroscopy can be supplemented by FTIR, which can detect the changes in functional groups on a plastic surface. In our study, a series of peaks in the 3000–3900 cm^{-1} region usually appeared in the IR spectra of weathered microplastics (Fig. S8), indicating the presence of O—H or N—H stretching vibrations. The broad peak at approximately 3360 cm^{-1} is the absorption peak of the associated hydroxyl group, and the presence of O—H indicates that hydrolytic and oxidizing processes occurred on the surface.

For PP and PE, the peaks at 1680–1800 cm^{-1} indicate carbonyl stretching vibrations, while a broad peak at 1010 cm^{-1} indicates C—O stretching vibrations. The carbonyl groups include amide, ketone, aldehyde, ester, carboxylic acid, and acid halide (Fig. 2). The existence of C=C is documented by several peaks at approximately 1640 cm^{-1} and confirmed by the peaks of C=C wag vibrations at 874 and 911 cm^{-1}. The peaks at 1640–1670 cm^{-1} are possibly indicative of the presence of water that is likely to be absorbed on a heavily oxidized surface. The presence of oxygen-containing functional groups suggests that the plastic surface was oxidized, whereas the occurrence of C=C bonds is consistent with the cleavage of the polymer carbon chain. In addition, the presence of amino groups (Fig. 2) suggests the influence of possible microbial activities during weathering. The spectra at 1600–1800 cm^{-1} are generally consistent, and there is no significant difference between PP and PE (Fig. 2). The consistency of the spectra may indicate a uniform weathering process for PP and PE.

The initial spectra of standard PVC and PET (Figs. S5, S6) are more complicated than those of PE and PP, and it is difficult to compare the spectra between standard plastics and weathered plastics. The carbon chain of PVC did not include carbonyl groups, but the carbonyl groups at 1717 cm^{-1} were detected in the spectra of standard PVC (Fig. S6), which might be related to the additives incorporated in the production process (Rahman and Brazel, 2004). The carbon chain of PVC originally includes the ketone carbonyl. The FTIR spectra of PVC and PET provide less information about the weathering process than do the spectra of PE and PP.

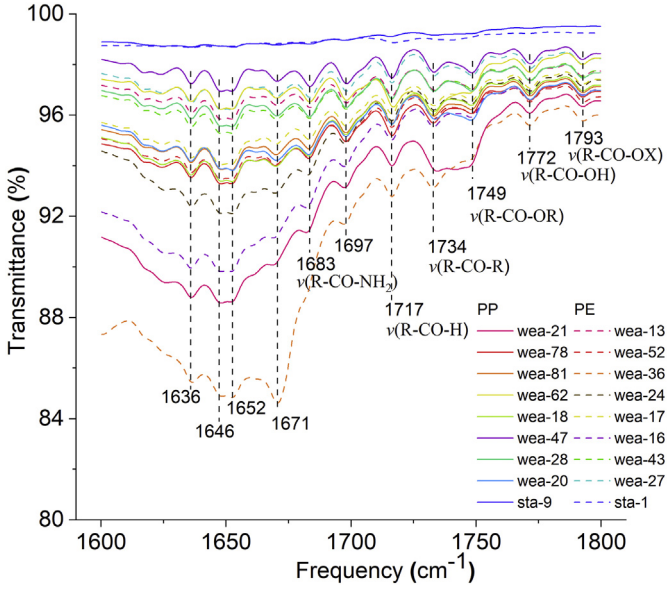

Fig. 2. FTIR spectra of PE and PP in the range of 1600–1800 cm^{-1}.

Compared with the FTIR spectra obtained after simulating the photooxidation process of plastics in the laboratory (Gardette et al., 2013; Jelle and Nilsen, 2011; Rouillon et al., 2016), the FTIR spectra in this study are complicated and informative. The ultraviolet (UV) radiation exposure experiments performed by Jelle and Nilsen (2011) showed two peaks at 1713 and 1732 cm^{-1} for PE and PP. Similarly, Rouillon et al. (2016) observed two peaks at 1712 and 1735 cm^{-1} in the photooxidation experiments of PP. Even the FTIR spectra of plastics in the environment (Cooper and Corcoran, 2010; Veerasingam et al., 2016; Zbyszewski and Corcoran, 2011; Zheng et al., 2019; Zhu et al., 2019) usually show only one or two peaks in the range of 1680–1800 cm^{-1}. In contrast, a series of peaks ranging from 1680 to 1800 cm^{-1} were observed in this study (Fig. 2) and may indicate that the plastic debris underwent complex physical-chemical weathering processes. In particular, the emergence of amino groups indicates that microbes may be involved in the weathering process.

3.4. Changes in surface morphology

The surface of the standard plastics is flat and smooth (Fig. S10), while the surface of the weathered plastics is rough and irregular with cracks, fractures, notching, pits, bumps and many small fragments or debris (Figs. 3 and S10). The surface of wea-16 (Fig. 3c, d) shows an interesting phenomenon. The surface of wea-16 has regular cracks similar to mud cracks (Fig. 3c), and there seems to be a layered weathering process on the plastic surface (Fig. 3d). The surface of this plastic debris was weathered and cracked; then, the debris peeled off from the initial surface and showed a wavy distribution while exposing a smooth inner surface. The small debris spilled from the initial surface might become smaller-sized microplastics; thus, we need to consider the smaller-sized microplastics in submicron- to microsized microplastics in the environment.

There are morphological differences between the weathered surfaces of PE (Fig. 3a–d) and those of PP (Fig. 3e–h). The weathered surface of PP has more pits, deeper cracks, and more prominent irregularities, while the weathered surface of PE is relatively smooth. In particular, rifts usually appear on the surfaces of PP rather than on the surfaces of PE (Fig. 3e, g). Therefore, compared to PP, PE is relatively more resistant to weathering processes. Cooper and Corcoran (2010) found that PE has more pits and fractures than does PP on the beaches of Hawaii and proposed that PE is more susceptible to oxidation than is PP, which contradicts our results. However, PE was more resistant to weathering than was PP on the beaches of Lake Huron, and this was explained as resulting from the difference in water chemistries between the beaches of Hawaii and those of Lake Huron (Zbyszewski and Corcoran, 2011). From the perspective of photochemical oxidation, the stability of PP is lower than that of PE because the carbon atoms in PP are tertiary carbons, which are more vulnerable to free radical attack (Andrady, 2017; Gewert et al., 2015). This perspective is consistent with our SEM results and the results in Lake Huron (Zbyszewski and Corcoran, 2011) but inconsistent with the results from the beaches of Hawaii (Cooper and Corcoran, 2010), which may reveal the impact of

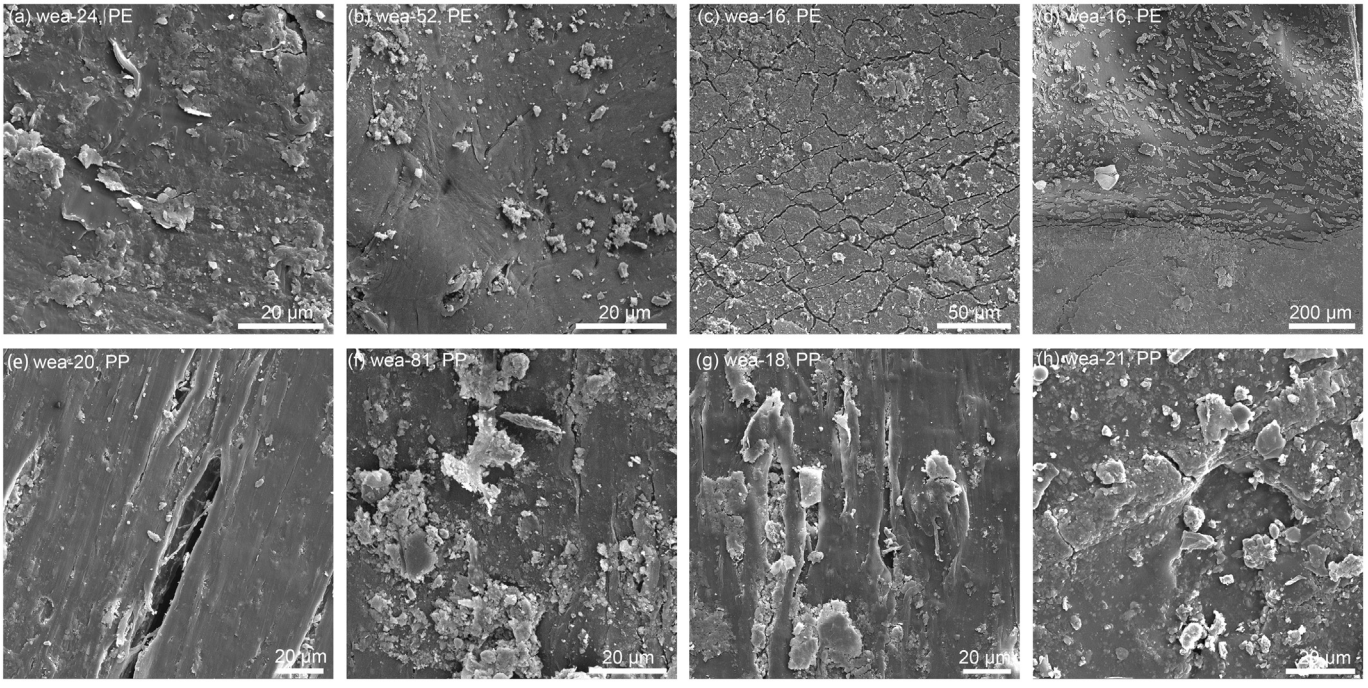

Fig. 3. Secondary electron images of weathered PE and PP.

natural geographical conditions on the differential weathering processes of PE and PP.

Changes in the surface O/C ratio.

The O atomic of the microplastic surface has a significant linear correlation with the C atomic (Fig. 4), which indicates the oxidation process on the surface. The O/C ratio of fresh standard microplastics is lower than the O/C ratio of weathered microplastics (Table S2). The increasing O/C ratio corresponds with the appearance of peaks associated with oxygen-containing functional groups in the FTIR spectra (Fig. 2). In addition, the O/C ratio is not consistent (Fig. 4) for different points for the same microplastic debris, which explains the heterogeneous oxidation process that occurred on the surface.

The O/C ratio of weathered microplastics is significantly related to the polymer types. The average O/C ratios for weathered PE and PP are 0.177 and 0.228, respectively. The O/C ratio of PP is higher than that of PE in the frequency distribution (Fig. 4), which corresponds with the SEM data (Fig. 3) and indicates that PP is more sensitive to oxidization processes than is PE. The generally identical functional groups on the weathered surface of PP and PE explain the consistent weathering process between PP and PE, but the differences in the SEM data and O/C ratio indicate a difference in weathering degree and further indicate a difference in resistance to weathering between PP and PE.

EDS was used to map the elemental composition of the wea-16 surface (Figs. 5 and S11), and the results show that the weathered outer surface has a high O content and a low C content, while the smooth internal surface has a low O content and a high C content. The EDS mappings of O and C are opposite and complementary, and both are consistent with the distribution of the weathered layer shown in the SEM. The O/C ratio of the weathered outer surface is approximately 0.1–0.5, and the O/C ratio of the inner surface without weathering is 0.01–0.03.

Unlike the initial O/C ratio of PE and PP, which is close to zero, the initial O/C ratios of PVC and PET are 0.045 ± 0.011 and 0.293 ± 0.082, respectively. The latter values correspond with the keto carbonyl group in the FTIR spectra of standard PVC and PET. The O and C atomic of weathered PVC and PET have a significant linear correlation (Fig. 4b, c), and the O/C ratio of weathered PVC and PET is significantly increased (Table S2). Therefore, we believe that the O/C ratio is a potential indicator to semiquantitatively determine the oxidation degree.

Changes in the O/C ratio on the surface of microplastics during the aging process of heat-activated $K_2S_2O_8$ and the Fenton treatment suggested that the O/C ratio can be used to reflect the oxidation degree (Liu et al., 2019b). The O/C ratio increased with aging time but tended to reach a plateau in the later period of aging. The changes in the O/C ratio were significantly related to the chemical oxidation method, and the O/C ratios of PE aged by heat-activated $K_2S_2O_8$ and the Fenton treatment after one month were 0.25 and 0.12, respectively (Liu et al., 2019b). However, the O/C ratio of microplastics weathered in natural conditions has a more alterable range (Fig. 4), which shows the complexity and persistence of the weathering process that occurs in the natural environment.

The O/C ratio for different locations on the same weathered microplastic debris is alterable (Figs. 5 and S11), and it is essential to collect multiple points on the same samples for a comprehensive assessment when using EDS to obtain the O/C ratio and assess the oxidization degree. Considering the different resistances to weathering in different polymer types, the O/C ratio might not be suitable for assessing the weathering degree and reflecting the decline in mechanical properties between different polymer types. Overall, the O/C ratio is a potential and convenient indicator of oxidation degree because collecting O/C data with SEM-EDS is practical and effective.

3.5. Titanium dioxide additives

We noticed the presence of titanium (Ti) on some surfaces of PVC and PET (Fig. S12), and Ti may be related to the titanium dioxide (TiO_2) that is used as a light-blocking aid and added in plastic production (Yang et al., 2004). TiO_2 is generally considered to have low toxicity (Skocaj et al., 2011), but nanosized or ultrafine TiO_2 (UF-TiO_2) (<100 nm in diameter) is genotoxic and cytotoxic to cultured human lymphoblastoid cells (Wang et al., 2007). Nanoplastics and microplastics are potential carriers of TiO_2 because TiO_2 is a common additive in many personal cares or consumer products (Weir et al., 2012).

Therefore, when evaluating the toxicity and health risks of microplastics, it is necessary to consider the inorganic or organic processing aids added during the plastic production process and carefully evaluate the composite pollution of these additives and microplastics or the leakage possibility (Schrank et al., 2019) of these additives in

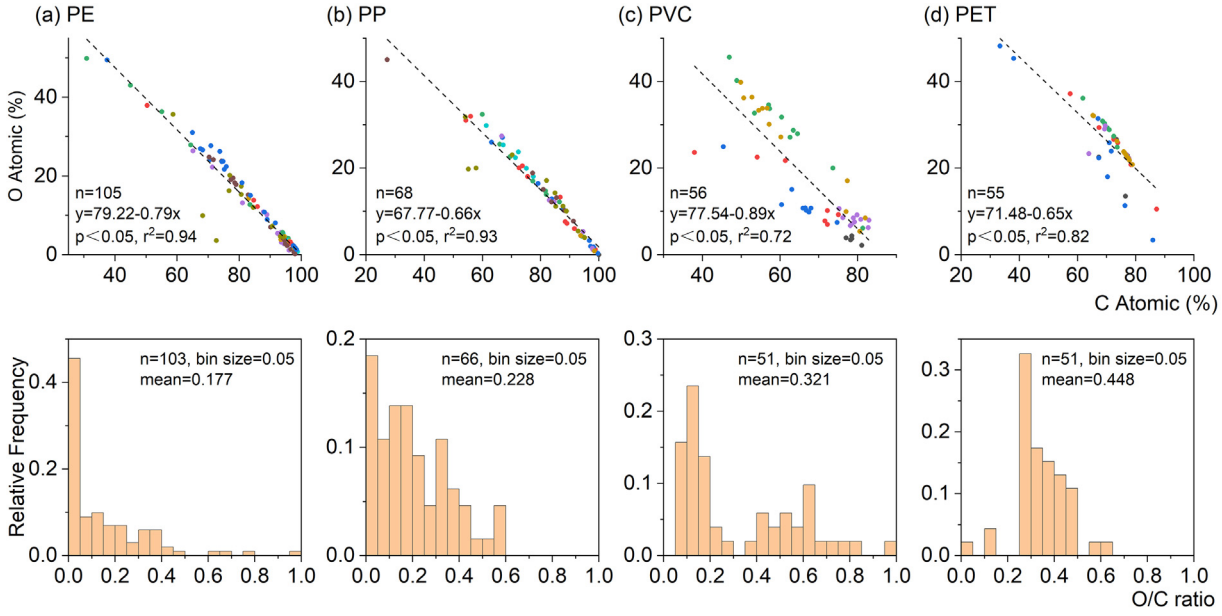

Fig. 4. Linear correlation between O and C atomic and frequency histogram of the O/C ratio. The values of the standard samples are included in the scatter graphs but excluded in the histograms. The different colors in the scatter graph represent different samples, and the multiple points of the same color represent different locations on the same sample.

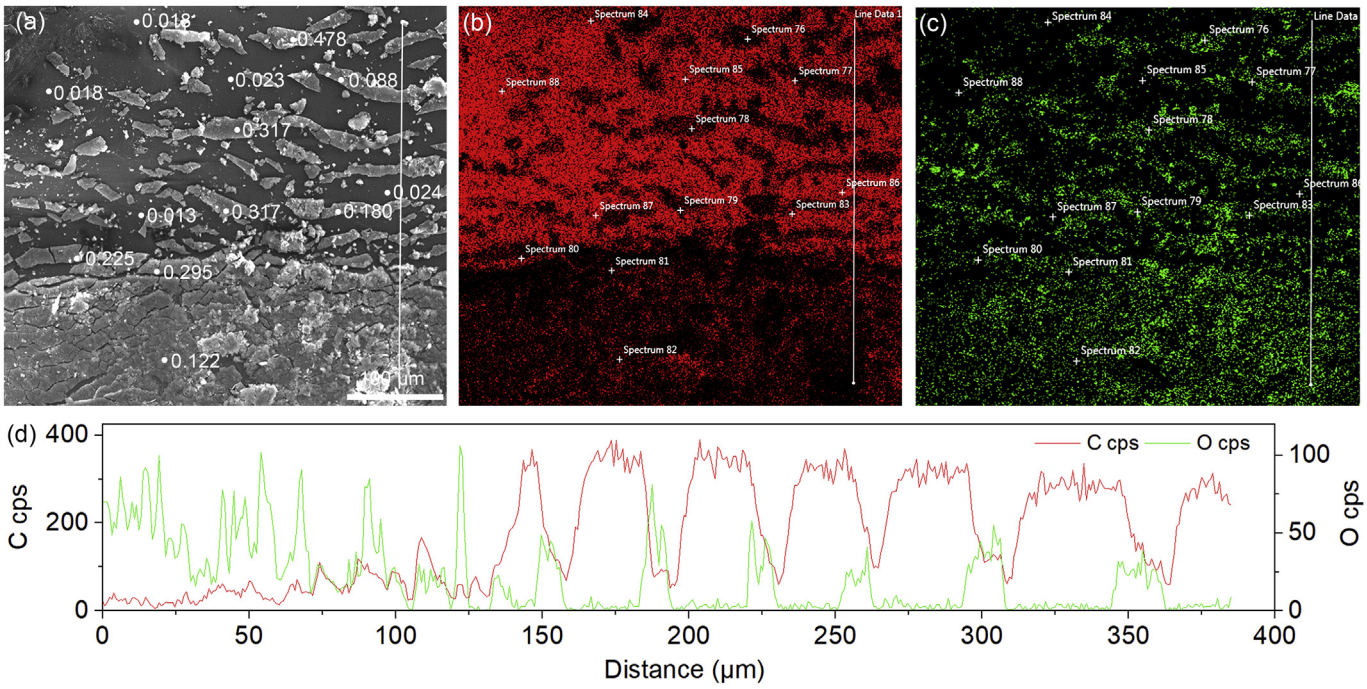

Fig. 5. Secondary electron image (a), EDS elemental maps (b: C map; c: O map) and line scan (d) of wea-16. The spectra of points were collected, and the O/C ratio for each point is marked in a.

the weathering process. In addition, in toxicological experiments on microplastics, the influence of microplastics itself and that of additives should be distinguished. The type of additive is related to the type of polymer, and we must accurately identify the polymer types.

3.6. Degradation of microplastics under natural conditions

Plastics are generally considered to be difficult to degrade, but a series of surface changes (Figs. 2 and 3) indicate obvious degradation of weathered microplastics in the sediments, and we still lack studies on plastic degradation in the long term (on the scales of decades). Microplastic is a potential indicator of the Anthropocene (Dong et al., 2020a; Zalasiewicz et al., 2016), but the surface changes and degradation will influence the environmental lifetime of microplastics and determine whether microplastics can serve as an indicator of the Anthropocene. The sediments (Fig. S1) were directly exposed to the atmosphere with sufficient sunlight and oxygen, and photooxidation may be the primary route of degradation (Gewert et al., 2015; Singh and Sharma, 2008). The mechanism of photooxidative degradation for polymers with a carbon-carbon backbone, such as PE, PP, PS and PVC, involves mainly the auto-oxidation cycle caused by free radical reactions (Gewert et al., 2015; Singh and Sharma, 2008). Moreover, hydrolytic degradation may occur on the basis of photooxidative degradation for polymers with heteroatoms in the main chain, such as PET and PA (Gewert et al., 2015). Biodegradation may occur later than abiotic degradation (Gewert et al., 2015; Shah et al., 2008). Studies have reported the interaction of microplastics with microbes or the biodegradation of microplastics in the marine environment (Roager and Sonnenschein, 2019; Syranidou et al., 2017; Zettler et al., 2013); however, currently, there is no study on the biodegradation of microplastics in terrestrial ecosystems such as soils or sediments.

Raman spectra of weathered microplastics have changed significantly compared to the standard spectra, but the mechanism underlying the relation of the changes in Raman spectra and the degradation of the microplastics must be further studied. The surface changes may be the reason for the variable Raman spectra of weathered microplastics. Changes in surface functional groups, surface oxidation and the cleavage of the carbon chain may lead to the attenuation of relevant peaks in Raman spectra. However, it is difficult to build or describe quantitative correlation among spectra, surface morphology and weathering time of environmental samples (Andrady, 2017). Whether a quantitative relation can be established between the changes in Raman spectra and the degree of oxidation and whether we can quantitively evaluate the degradation or surface changes of weathered microplastics through Raman spectra are important issues to be considered in the future. FTIR could reveal changes in surface functional groups, SEM-EDS could reveal changes in surface morphology and elements distribution, and Raman would be influenced by surface changes as well. FTIR, SEM-EDS and Raman could complement each other. Combined spectral and elemental analyses can be useful in deciphering the degradation processes of microplastics weathered under natural conditions.

4. Conclusion

The Raman spectra of weathered microplastics are distinctly different from the spectra of fresh standard samples, and many peaks in the Raman spectra of weathered microplastics are weakened and even invisible. A Raman database of weathered microplastics was established to specifically identify the polymer types of weathered microplastics. Carbon-carbon double bonds and a series of carbonyl groups appeared on the surface of weathered microplastics, which indicates the cleavage of the carbon chain and oxidation process. The weathered microplastics have rougher surfaces and a higher O/C ratio than the standard samples. The complementary C and O elemental maps suggested that the O/C ratio is a potential indicator of oxidation degree.

Abbreviations

wea-n	weathered microplastic debris
sta-n	standard microplastic debris and particles
PP	polypropylene
PE	polyethylene
NC	nitrocellulose
PVC	polyvinyl chloride

PET	polyester
PA	polyamine (nylon)
PC	polycarbonate
ABS	acrylonitrile butadiene styrene

CRediT authorship contribution statement

Mingtan Dong: Conceptualization, Methodology, Formal analysis, Investigation, Writing - original draft. **Qiaoqiao Zhang:** Investigation, Software, Formal analysis, Writing - original draft. **Xinli Xing:** Methodology, Formal analysis, Writing - review & editing. **Wei Chen:** Validation, Formal analysis, Writing - review & editing. **Zhenbing She:** Methodology, Resources, Writing - review & editing. **Zejiao Luo:** Supervision, Project administration, Funding acquisition, Writing - review & editing.

Declaration of competing interest

The authors declare that they have no known competing financial interests or personal relationships that could have appeared to influence the work reported in this paper.

Acknowledgments

We acknowledge Zhihang Ye, Yue Sun and Mingying Shao for their assistance in the field sampling and laboratory work. This study was supported by the National Key Research and Development Program of China (No. 2017YFD0801005), the National Natural Science Foundation of China (No. 41672246), and the Fund for Hubei Technology Innovation (No. 2017ACA092).

Appendix A. Supplementary data

Introduction of the study area and the location of sampling sites; Raman and FTIR spectra of weathered microplastic debris; Supplemental secondary electron images and the EDS elemental analysis; Carbonyl index and hydroxyl index of microplastics weathered under natural conditions (PDF).

Research data

Supplemental dataset of the Raman database of weathered microplastics

Dong, M., Zhang, Q., Xing, X., Chen, W., She, Z., Luo, Z., 2020c. A Raman database of microplastics weathered under natural environments. Mendeley Data, V2, doi: 10.17632/kpygrf9fg6.2. Supplementary data to this article can be found online at https://doi.org/10.1016/j.scitotenv.2020.139990.

References

Andrady, A.L., 2017. The plastic in microplastics: a review. Mar. Pollut. Bull. 119, 12–22.

Brandon, J.A., Freibott, A., Sala, L.M., Patterns of suspended and salp-ingested microplastic debris in the North Pacific investigated with epifluorescence microscopy. Limnol. Oceanogr. Lett..

Chain, E.Panel o.C.i.t.F, 2016. Presence of microplastics and nanoplastics in food, with particular focus on seafood. EFSA J. 14, e04501.

Cooper, D.A., Corcoran, P.L., 2010. Effects of mechanical and chemical processes on the degradation of plastic beach debris on the island of Kauai, Hawaii. Mar. Pollut. Bull. 60, 650–654.

Dehaut, A., Hermabessiere, L., Duflos, G., 2019. Current frontiers and recommendations for the study of microplastics in seafood. TrAC Trends Anal. Chem. 116, 346–359.

Di, M., Liu, X., Wang, W., Wang, J., 2019. Manuscript prepared for submission to environmental toxicology and pharmacology pollution in drinking water source areas: microplastics in the Danjiangkou reservoir, China. Environ. Toxicol. Pharmacol. 65, 82–89.

Dong, M., Luo, Z., Jiang, Q., Xing, X., Zhang, Q., Sun, Y., 2020a. The rapid increases in microplastics in urban lake sediments. Sci. Rep. 10, 848.

Dong, M., Zhang, Q., Xing, X., Chen, W., She, Z., Luo, Z., 2020c. A Raman database of microplastics weathered under natural environments. Mendeley Data, V2 https://doi.org/10.17632/kpygrf9fg6.2.

Dong, Y., Gao, M., Song, Z., Qiu, W., 2020b. As(III) adsorption onto different-sized polystyrene microplastic particles and its mechanism. Chemosphere 239, 124792.

Gao, F., Li, J., Sun, C., Zhang, L., Jiang, F., Cao, W., Zheng, L., 2019. Study on the capability and characteristics of heavy metals enriched on microplastics in marine environment. Mar. Pollut. Bull. 144, 61–67.

Gardette, M., Perthue, A., Gardette, J.-L., Janecska, T., Földes, E., Pukánszky, B., Therias, S., 2013. Photo- and thermal-oxidation of polyethylene: comparison of mechanisms and influence of unsaturation content. Polym. Degrad. Stab. 98, 2383–2390.

Gewert, B., Plassmann, M.M., MacLeod, M., 2015. Pathways for degradation of plastic polymers floating in the marine environment. Environ Sci Process Impacts 17, 1513–1521.

Gray, A.D., Weinstein, J.E., 2017. Size- and shape-dependent effects of microplastic particles on adult daggerblade grass shrimp (Palaemonetes pugio). Environ. Toxicol. Chem. 36, 3074–3080.

Huang, Y., Yan, M., Xu, K., Nie, H., Gong, H., Wang, J., 2019. Distribution characteristics of microplastics in Zhubi reef from South China Sea. Environ. Pollut. 255.

Huffer, T., Weniger, A.K., Hofmann, T., 2018. Sorption of organic compounds by aged polystyrene microplastic particles. Environ. Pollut. 236, 218–225.

Imhof, H.K., Laforsch, C., Wiesheu, A.C., Schmid, J., Anger, P.M., Niessner, R., Ivleva, N.P., 2016. Pigments and plastic in limnetic ecosystems: a qualitative and quantitative study on microparticles of different size classes. Water Res. 98, 64–74.

Jelle, B.P., Nilsen, T.-N., 2011. Comparison of accelerated climate ageing methods of polymer building materials by attenuated total reflectance Fourier transform infrared radiation spectroscopy. Constr. Build. Mater. 25, 2122–2132.

Kappler, A., Fischer, D., Oberbeckmann, S., Schernewski, G., Labrenz, M., Eichhorn, K.J., Voit, B., 2016. Analysis of environmental microplastics by vibrational microspectroscopy: FTIR, Raman or both? Anal. Bioanal. Chem. 408, 8377–8391.

Koelmans, A.A., Besseling, E., Wegner, A., Foekema, E.M., 2013. Plastic as a carrier of POPs to aquatic organisms: a model analysis. Environ. Sci. Technol. 47, 7812–7820.

Li, L., Geng, S., Wu, C., Song, K., Sun, F., Visvanathan, C., Xie, F., Wang, Q., 2019. Microplastics contamination in different trophic state lakes along the middle and lower reaches of Yangtze River basin. Environ. Pollut. 254 (Part A), 112951.

Liu, J., Zhang, T., Tian, L., Liu, X., Qi, Z., Ma, Y., Ji, R., Chen, W., 2019a. Aging significantly affects mobility and contaminant-mobilizing ability of nanoplastics in saturated loamy sand. Environ. Sci. Technol. 53, 5805–5815.

Liu, P., Qian, L., Wang, H., Zhan, X., Lu, K., Gu, C., Gao, S., 2019b. New insights into the aging behavior of microplastics accelerated by advanced oxidation processes. Environ. Sci. Technol. 53, 3579–3588.

Miraj, S.S., Parveen, N., Zedan, H.S., 2019. Plastic microbeads: small yet mighty concerning. Int. J. Environ. Health Res. 1–17.

Ossmann, B.E., Sarau, G., Holtmannspotter, H., Pischetsrieder, M., Christiansen, S.H., Dicke, W., 2018. Small-sized microplastics and pigmented particles in bottled mineral water. Water Res. 141, 307–316.

Pico, Y., Alfarhan, A., Barcelo, D., 2019. Nano- and microplastic analysis: focus on their occurrence in freshwater ecosystems and remediation technologies. TrAC Trends Anal. Chem. 113, 409–425.

Rahman, M., Brazel, C., 2004. The plasticizer market: an assessment of traditional plasticizers and research trends to meet new challenges. Prog. Polym. Sci. 29, 1223–1248.

Roager, L., Sonnenschein, E.C., 2019. Bacterial candidates for colonization and degradation of marine plastic debris. Environ. Sci. Technol. 53, 11636–11643.

Roch, S., Walter, T., Ittner, L.D., Friedrich, C., Brinker, A., 2019. A systematic study of the microplastic burden in freshwater fishes of south-western Germany - are we searching at the right scale? Sci. Total Environ. 689, 1001–1011.

Rouillon, C., Bussiere, P.O., Desnoux, E., Collin, S., Vial, C., Therias, S., Gardette, J.L., 2016. Is carbonyl index a quantitative probe to monitor polypropylene photodegradation? Polym. Degrad. Stab. 128, 200–208.

Schrank, I., Trotter, B., Dummert, J., Scholz-Bottcher, B.M., Loder, M.G.J., Laforsch, C., 2019. Effects of microplastic particles and leaching additive on the life history and morphology of Daphnia magna. Environ. Pollut. 255, 113233.

Schwaferts, C., Niessner, R., Elsner, M., Ivleva, N.P., 2019. Methods for the analysis of submicrometer- and nanoplastic particles in the environment. TrAC Trends Anal. Chem. 112, 52–65.

Shah, A.A., Hasan, F., Hameed, A., Ahmed, S., 2008. Biological degradation of plastics: a comprehensive review. Biotechnol. Adv. 26, 246–265.

Singh, B., Sharma, N., 2008. Mechanistic implications of plastic degradation. Polym. Degrad. Stab. 93, 561–584.

Skocaj, M., Filipic, M., Petkovic, J., Novak, S., 2011. Titanium dioxide in our everyday life; is it safe? Radiol. Oncol. 45, 227–247.

Sobhani, Z., Al Amin, M., Naidu, R., Megharaj, M., Fang, C., 2019. Identification and visualisation of microplastics by Raman mapping. Anal. Chim. Acta 1077, 191–199.

Sobhani, Z., Zhang, X., Gibson, C., Naidu, R., Megharaj, M., Fang, C., 2020. Identification and visualisation of microplastics/nanoplastics by Raman imaging (i): down to 100 nm. Water Res. 174.

Song, Y.K., Hong, S.H., Eo, S., Jang, M., Han, G.M., Isobe, A., Shim, W.J., 2018. Horizontal and vertical distribution of microplastics in Korean coastal waters. Environ. Sci. Technol. 52, 12188–12197.

Strungaru, S.-A., Jijie, R., Nicoara, M., Plavan, G., Faggio, C., 2019. Micro- (nano) plastics in freshwater ecosystems: abundance, toxicological impact and quantification methodology. TrAC Trends Anal. Chem. 110, 116–128.

Syranidou, E., Karkanorachaki, K., Amorotti, F., Franchini, M., Repouskou, E., Kaliva, M., Vamvakaki, M., Kolvenbach, B., Fava, F., Corvini, P.F., Kalogerakis, N., 2017. Biodegradation of weathered polystyrene films in seawater microcosms. Sci. Rep. 7, 17991.

Thompson, R.C., Olsen, Y., Mitchell, R.P., Davis, A., Rowland, S.J., John, A.W., McGonigle, D., Russell, A.E., 2004. Lost at sea: where is all the plastic? Science 304, 838.

Tosin, M., Weber, M., Siotto, M., Lott, C., Degli Innocenti, F., 2012. Laboratory test methods to determine the degradation of plastics in marine environmental conditions. Front. Microbiol. 3, 225.
Veerasingam, S., Saha, M., Suneel, V., Vethamony, P., Rodrigues, A.C., Bhattacharyya, S., Naik, B.G., 2016. Characteristics, seasonal distribution and surface degradation features of microplastic pellets along the Goa coast, India. Chemosphere 159, 496–505.
Vianello, A., Jensen, R.L., Liu, L., Vollertsen, J., 2019. Simulating human exposure to indoor airborne microplastics using a breathing thermal manikin. Sci. Rep. 9.
Wang, J.J., Sanderson, B.J., Wang, H., 2007. Cyto- and genotoxicity of ultrafine TiO2 particles in cultured human lymphoblastoid cells. Mutat. Res. 628, 99–106.
Wang, W., Yuan, W., Chen, Y., Wang, J., 2018. Microplastics in surface waters of Dongting Lake and Hong Lake, China. Sci. Total Environ. 633, 539–545.
Weir, A., Westerhoff, P., Fabricius, L., Hristovski, K., von Goetz, N., 2012. Titanium dioxide nanoparticles in food and personal care products. Environ. Sci. Technol. 46, 2242–2250.
Xiong, X., Zhang, K., Chen, X., Shi, H., Luo, Z., Wu, C., 2018. Sources and distribution of microplastics in China's largest inland lake - Qinghai Lake. Environ. Pollut. 235, 899–906.
Yang, H., Zhu, S., Pan, N., 2004. Studying the mechanisms of titanium dioxide as ultraviolet-blocking additive for films and fabrics by an improved scheme. J. Appl. Polym. Sci. 92, 3201–3210.
Zalasiewicz, J., Waters, C.N., Ivar do Sul, J.A., Corcoran, P.L., Barnosky, A.D., Cearreta, A., Edgeworth, M., Gałuszka, A., Jeandel, C., Leinfelder, R., McNeill, J.R., Steffen, W., Summerhayes, C., Wagreich, M., Williams, M., Wolfe, A.P., Yonan, Y., 2016. The geological cycle of plastics and their use as a stratigraphic indicator of the Anthropocene. Anthropocene 13, 4–17.
Zarfl, C., 2019. Promising techniques and open challenges for microplastic identification and quantification in environmental matrices. Anal. Bioanal. Chem. 411, 3743–3756.
Zbyszewski, M., Corcoran, P.L., 2011. Distribution and degradation of fresh water plastic particles along the beaches of Lake Huron, Canada. Water Air Soil Pollut. 220, 365–372.
Zettler, E.R., Mincer, T.J., Amaral-Zettler, L.A., 2013. Life in the "plastisphere": microbial communities on plastic marine debris. Environ. Sci. Technol. 47, 7137–7146.
Zhang, H., Wang, J., Zhou, B., Zhou, Y., Dai, Z., Zhou, Q., Chriestie, P., Luo, Y., 2018. Enhanced adsorption of oxytetracycline to weathered microplastic polystyrene: kinetics, isotherms and influencing factors. Environ. Pollut. 243, 1550–1557.
Zheng, Y., Li, J., Cao, W., Liu, X., Jiang, F., Ding, J., Yin, X., Sun, C., 2019. Distribution characteristics of microplastics in the seawater and sediment: a case study in Jiaozhou Bay, China. Sci. Total Environ. 674, 27–35.
Zhu, J., Zhang, Q., Li, Y., Tan, S., Kang, Z., Yu, X., Lan, W., Cai, L., Wang, J., Shi, H., 2019. Microplastic pollution in the Maowei Sea, a typical mariculture bay of China. Sci. Total Environ. 658, 62–68.
Zuccarello, P., Ferrante, M., Cristaldi, A., Copat, C., Grasso, A., Sangregorio, D., Fiore, M., Oliveri Conti, G., 2019. Exposure to microplastics (<10mum) associated to plastic bottles mineral water consumption: the first quantitative study. Water Res. 157, 365–371.